IEEE Photonics Journal
An IEEE Photonics Society Publication

Open Access

Ultrabroadband Polarization-Insensitive Coupler Based on Dual-Core Photonic Crystal Fiber

Volume 9, Number 1, February 2017

Tongtong Zhao
Shuqin Lou
Xin Wang
Min Zhou
Zhenggang Lian

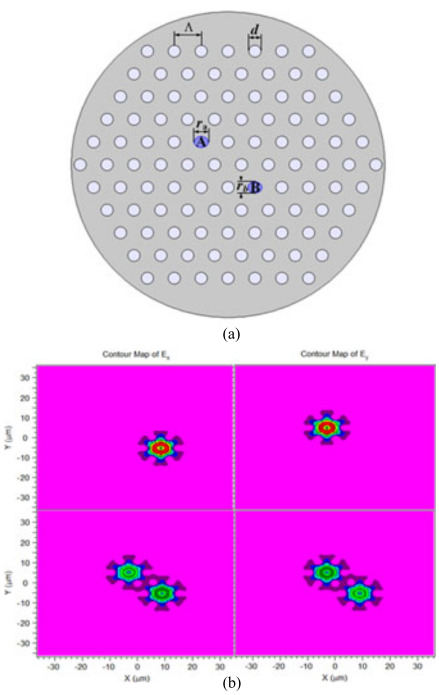

DOI: 10.1109/JPHOT.2016.2644864

Ultrabroadband Polarization-Insensitive Coupler Based on Dual-Core Photonic Crystal Fiber

Tongtong Zhao,[1] Shuqin Lou,[1] Xin Wang,[1] Min Zhou,[1] and Zhenggang Lian[2]

[1]School of Electronic and Information Engineering, Beijing Jiaotong University, Beijing 100044, China
[2]Yangtze Optical Electronic Co., Wuhan 430000, China

DOI:10.1109/JPHOT.2016.2644864

Manuscript received December 2, 2016; revised December 18, 2016; accepted December 21, 2016. Date of publication January 18, 2017; date of current version January 26, 2017. This work was supported in part by the National Natural Science Foundation of China under Grant 61475016 and Grant 61575016 and in part by the key project of China Railway Corporation under Grant 2016J006-E. Corresponding author: S. Lou (e-mail: shqlou@bjtu.edu.cn).

Abstract: We propose a dual-core photonic crystal fiber (PCF) for a broad bandwidth polarization-insensitive coupler. To achieve ultrabroadband and polarization-insensitive characteristics, two elliptical fluorine-doped cores are introduced. By optimizing structure parameters and fiber length, a polarization-insensitive 50:50 coupler is achieved. Its coupling ratio stabilizes at 50 $\pm$ 1% the in whole optical communication band from 1.255 to 1.725 μm, and the coupling ratio difference between two polarizations is lower than 0.2%. This coupler also has high compatibility with standard single-mode fibers (SMFs) due to low splice loss. Fabrication feasibility is improved due to the use of uniform circular air holes. Tolerance analysis results indicate that the designed coupler has great potential for practical fabrication. High fabrication feasibility and good performance give it great potential to be used in optical communication systems.

Index Terms: Photonic crystal fiber (PCF) coupler, polarization-insensitive, broad bandwidth, high compatibility.

1. Introduction

The optical directional coupler plays an important role in communication systems. Although it has already been commercially available, there are still some common problems for couplers based on conventional dual-core fibers, such as narrow bandwidth and polarization-sensitive [1], [2], which make the couplers hard to meet the requirements for a high rate, ultra-broadband communication system.

Compared with the conventional fiber couplers, the couplers based on photonic crystal fibers (PCFs) have the advantage on achieving broad bandwidth and polarization-insensitive characteristics [3], [4]. Currently, PCF-based couplers have attracted lots of attention. Early in 2000, the mode coupling behavior in dual-core PCF had been studied experimentally by Mangan *et al.* [5] for the first time. Since then, many directional couplers based on PCFs have been designed. For example, Lægsgaard *et al.* [6] designed a coupler by introducing two fluorine-doped cores in PCF in 2004. This fiber achieves a broad bandwidth covers from 0.75 μm to 1.5 μm. But the birefringence induced by the fluorine-doped cores makes the coupling ratio sensitive to polarization.

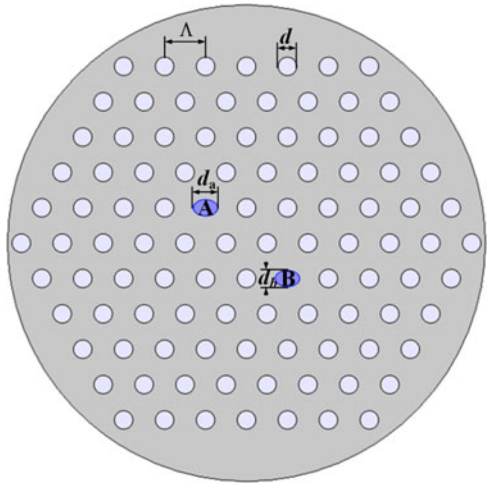

Fig. 1. Cross section of dual-core PCF.

In 2006, Varshney *et al.* [7] designed a dual-core PCF which achieved a broad bandwidth from 0.9 to 1.6 μm. But the air holes of this fiber are elliptical holes. It is very difficult to fabricate silica based PCF with uniform oriented elliptical air holes by using current fabrication process. Most recently, the coupling characteristics of a novel design with metal wire had been studied [8]. The extinction ratio can reach 30.54 dB at 1.55 μm, but the confinement loss of this fiber is extremely high.

Until now, many structures are proposed for achieving directional couplers with good performance, including PCFs with metal wires [3], [8], liquid crystal [9], elliptical air holes [10] or modulation core [11], and so on [12]–[14]. All the structures mentioned above have their own advantages, but most of these designs can not achieve a good performance with a simple structure. Moreover, the compatibility with practical optical communication systems also need to be taken into consideration since large mode field area (MFA) mismatch between PCF and single mode fiber (SMF) will lead to high splice loss [15]. And the short distance between two cores increases the difficulty of introducing input light and isolating output light.

Considering the fabrication and application, we propose a novel broad bandwidth polarization-insensitive PCF-based with two elliptical fluorine-doped cores. The proposed coupler can achieve an ultra-broad bandwidth covering the wavelength from 1.255 μm to 1.725 μm, i.e., all communication bands. And the difference of coupling ratio between two polarizations is lower than 0.2%. The proposed PCF with high performance and simple structure has great potential in developing a directional coupler for using in a high-rate, ultra-broadband communication system.

2. Structure and Principle

Fig. 1 shows the cross section of dual-core PCF. The gray section is pure silica host background. The white circles represent air holes. These air holes are arranged in triangular lattice with uniform diameter of d and holes pitch Λ. Two symmetrical cores, represented by A and B in Fig. 1, are formed by two elliptical fluorine-doped rods. The difference of refractive index between fluorine-doped core and silica is labeled by Δ. The major axis and minor axis diameter of elliptically fluorine-doped core are denoted by d_a and d_b, respectively, and the ellipticity can be defined as $e = d_a/d_b$.

The fiber properties are analyzed by adapting the full vector Finite element method (FEM) [16] combined with perfectly matched layer (PML) boundary conditions [17], which is widely used for simulating micro-structure fibers [18], [19]. A 5 μm-thick circular PML is set outside the cladding. High density meshes with the numbers of degrees of freedom in the range from 82 000 to 83 000 are used.

The designed dual-core coupler is based on the interaction of odd and even modes. The coupling length L_c, which shows the coupling strength between two cores, can be defined by [20]

$$L_c^{x,y} = \frac{\lambda}{2(n_e^{x,y} - n_o^{x,y})} \tag{1}$$

where λ is the free space wavelength, and $n_e^{x,y}$ and $n_o^{x,y}$ are effective indexes of even and odd modes. The polarization-insensitive can be achieved when lights with different polarizations have nearly same coupling length.

In dual-core fiber, the energy in one core will couples into another one when the light propagates along the fiber. After propagating for a length of L, the coupling ratio $C^{x,y}$ can be calculated by [20]

$$C_A^{x,y}(z) = \frac{P_{out,A}^{x,y}}{P_{in}^{x,y}} = \cos^2\left(\frac{\pi}{2}\frac{L}{L_c^{x,y}}\right)$$
$$C_B^{x,y}(z) = \frac{P_{out,B}^{x,y}}{P_{in}^{x,y}} = \sin^2\left(\frac{\pi}{2}\frac{L}{L_c^{x,y}}\right). \tag{2}$$

L is the propagation distance of coupling region. When the propagation distance is equal to $L_c/2$, the PCF can be used as a 50:50 coupler. For a 50:50 coupler, the maximum value of coupling ratio is 51% because that the accuracy of the coupling ratio should be controlled within $\pm 1\%$ [11]. Therefore, we assume that a coupler length L_0 satisfies the following equation:

$$L_0 = 2L_{\max} \arccos(\sqrt{0.51})/\pi \tag{3}$$

where $L_{\max}$ is the maximum value of the coupling length.

The coupling ratio difference C_Δ is introduced for discussing the polarization-insensitive characteristics of the coupler. It can be described as

$$C_\Delta^{x-y} = C_x - C_y. \tag{4}$$

3. Numerical results

In view of the application, the compatibility with other optical components in the communication system is very important for the design. So we choose SMFs as input and output ports, which makes the coupler connected easily with other optical fiber components. According to the coupled-mode theory, high splice loss will be introduced due to MFA mismatch, and the splice loss caused by MFA mismatch between PCF and SMF can be defined as [21]

$$L_m = -10 \lg\left[\left(\frac{2R_{pcf}R_{smf}}{R_{pcf}^2 + R_{smf}^2}\right)^2\right] \tag{5}$$

where R_{pcf} and R_{smf} are MFA radius of PCF and SMF, respectively.

We set the initial parameters of the proposed PCF as $d/\Lambda = 0.45$, $d_a/\Lambda = 0.45$, $d_b/\Lambda = 0.42$, and $\Delta = -1.3\%$. Fig. 2(a) shows the MFAs in one core with different Λ. It should be noted that the MFAs decrease with the increase of wavelength. This is caused by the anti-guiding phenomenon due to the introduction of fluorine-doped core [22]. The refractive index of fluorine-doped cores is lower than that, and therefore, so with the decrease of wavelength, the fundamental mode spreads out from the fluorine-doped core, leading to an increase in MFA, and the MFA at 1.55 μm is about 70 μm^2, which is close to the MFA of SMF. Fig. 2(b) shows the splice losses as function of air holes pitch Λ. It should be noted that the splice losses are very small when $\Lambda = 6\,\mu$m. So, we set $\Lambda = 6\,\mu$m. The splice loss caused by the mismatch of MFA is lower than 0.045 dB.

The elliptical fluorine-doped core makes the coupling coefficients in x- and y-polarizations extremely close. The core of this designed PCF is formed by elliptical fluorine-doped rod. Fig. 3 illustrates the change of coupling length with different e and d_b/Λ. Fig. 3(a) shows that both the

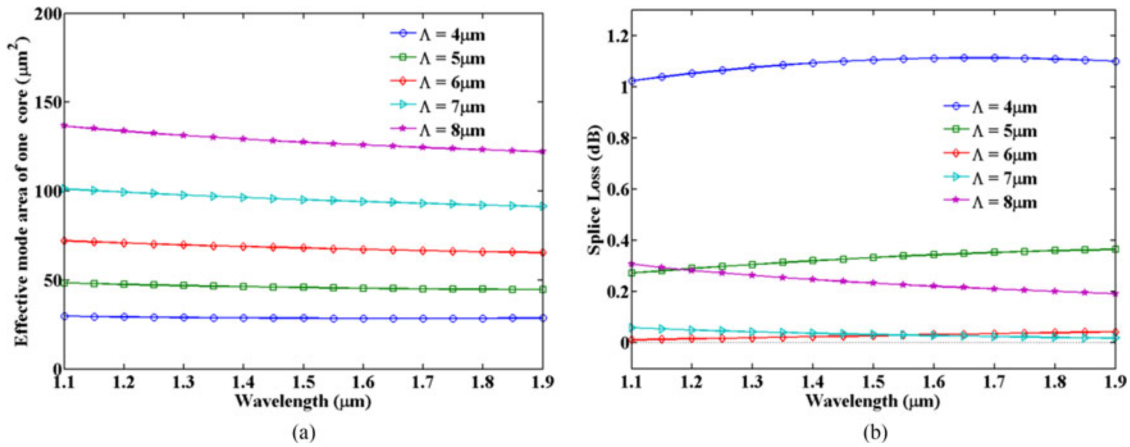

Fig. 2. MFAs of one core (a) and splice losses (b) with different Λ.

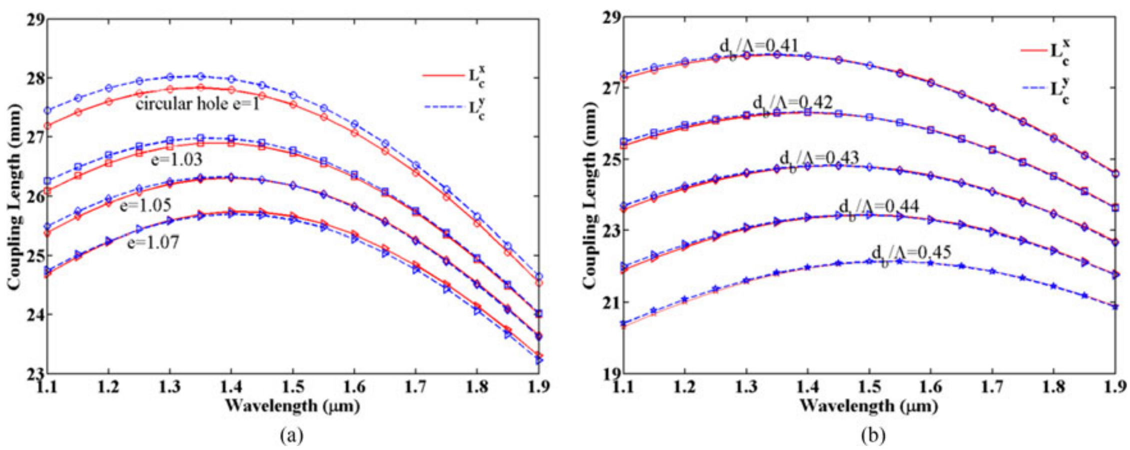

Fig. 3. Coupling length with different e (a) and d_b/Λ (b).

coupling length and coupling length difference become smaller when the elliptical cores are introduced. This is because that the introduction of the elliptical cores offset the geometric birefringence of the PCF. As show in Fig. 3(b), the minor axis diameter has slight effects on the coupling length difference between two polarizations, but the peak of coupling ratio shifts with the increase of the d_b. Considering the polarization-insensitive and working wavelength range, we set e = 1.05 and $d_b/\Lambda = 0.44$.

Fig. 4(a) shows the coupling ratios with different air holes diameter. The peak of the coupling ratio has a blue shift and the bandwidth becomes a little broader as air holes diameter increasing. The coupling ratio difference between two polarizations is shown in Fig. 4(b). It should be noted that the C_Δ is lower than 0.3% when the d/Λ is set as 0.45. It means that the proposed PCF coupler has good polarized insensitivity. Although the bandwidth becomes a little narrower than that of $d/\Lambda = 0.5$, the polarized insensitivity becomes much better. Therefore, in order to balance the bandwidth and the polarization-insensitivity, we set $d/\Lambda = 0.45$.

The coupling ratio and coupling ratio difference with different fluorine-doped concentration are shown in Fig. 5. It should be noted that the fluorine-doped concentration has slight effect on the coupling ratio difference, but it can regulate the working wavelength range of the coupler. The working wavelength range shifts to the longer wavelength and the bandwidth becomes broader with the increase of Δ. In order to achieve the broad bandwidth and reduce the fabrication difficulty, we set $\Delta = 1.3\%$.

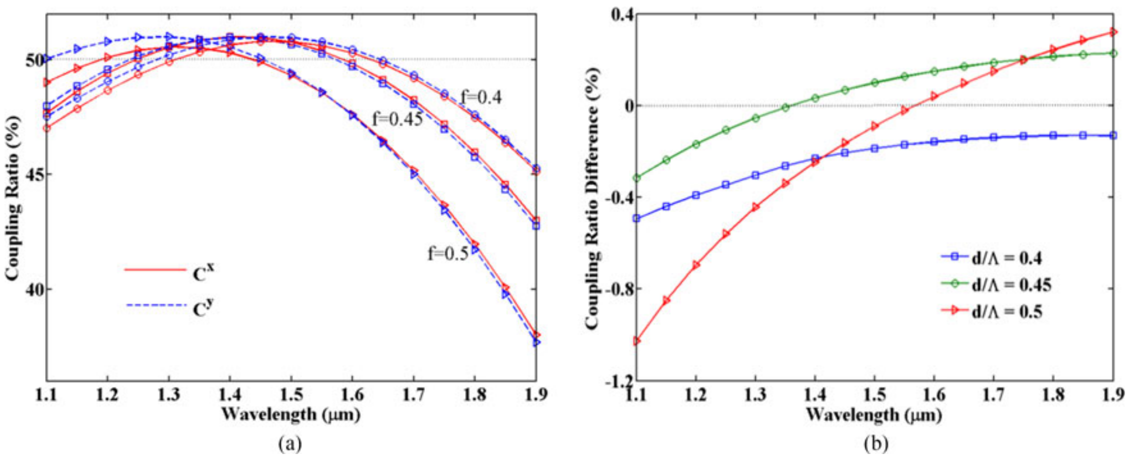

Fig. 4. Coupling ratio (a) and coupling ratio difference between two polarizations (b) with different d/Λ.

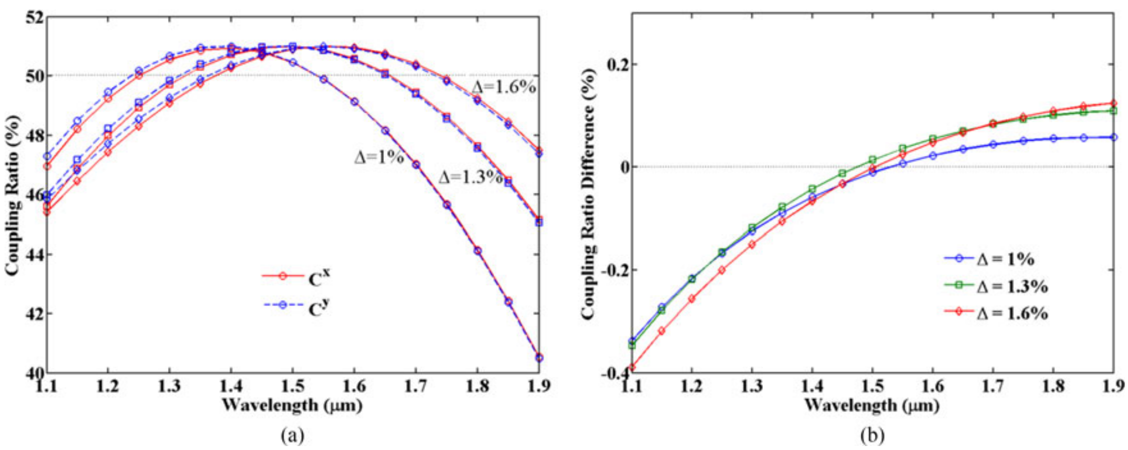

Fig. 5. Coupling ratio (a) and coupling ratio difference between two polarizations (b) with different Δ.

The coupling length, coupling ratio and coupling ratio difference between two polarizations are shown in Fig. 6. By using the designed fiber with the length of 11.6 mm, the coupling ratio can be controlled within 50 $\pm$ 1% in wavelength from 1.255 μm to 1.725 μm, which covers all communication bands, and the difference of coupling ratio between two polarizations is less than 0.2%. Numerical results demonstrate that the proposed dual-core PCF based coupler can achieve broad bandwidth and polarization-insensitive with $\Lambda = 6\,\mu$m, $d/\Lambda = 0.45$, $d_b/\Lambda = 0.44$, e = 1.05 and $\Delta = 1.3\%$.

We analyze the evolution process of the mode field by using full-vector beam propagation method (BPM) [23] to show the coupling mechanism of designed coupler. At Z = 0, the input lights in *x*- and *y*-polarizations are injected into core A and B, respectively. The evolution of mode field distribution at the wavelength of 1.55 μm is shown in Fig. 7. After propagating a distance of 11.6 mm, the electrical field energy of *x*-polarized and *y*-polarized light is almost same in two cores. Thus, two different polarization modes exist in the same core. In this way the coupling function is realized. These are consistent with the numerical result calculated by the full-vector FEM.

To verify the ultra-broad bandwidth characteristics of the proposed coupler, we analyze the evolution process of the electric field at the wavelengths of 1.255 μm and 1.725 μm. The evolutions of electric field along the fiber are shown in Fig. 8. It should be noted that the lights with different polarization will couple from core A to B with similar speed. After propagating the distance of

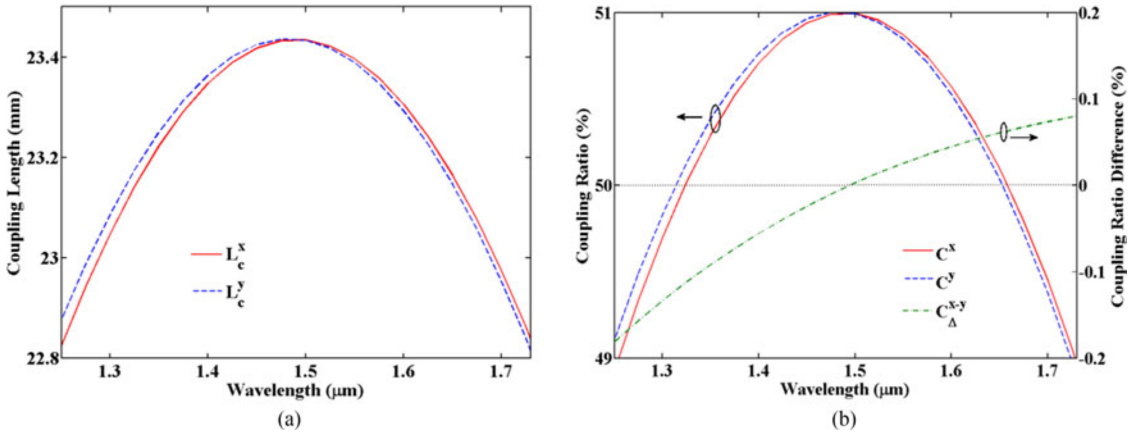

Fig. 6. Coupling length (a). Coupling ratio and coupling ratio difference between two polarizations (b).

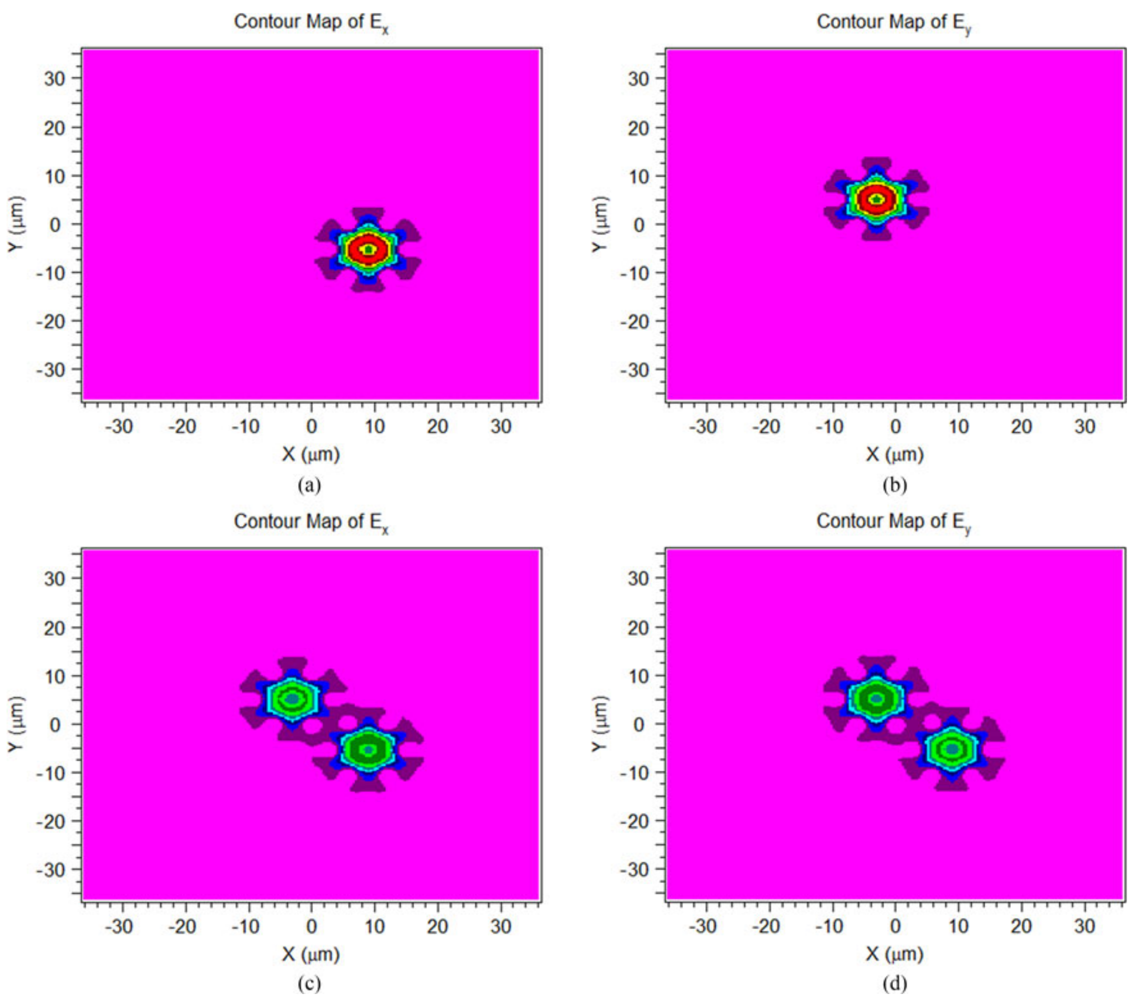

Fig. 7. Mode field distributions of *x*-polarization when $Z = 0$ (a) and $Z = 11.6\,\text{mm}$ (c). Mode field distributions of *y*-polarization when $Z = 0$ (b) and $Z = 11.6\,\text{mm}$ (d) and at 1.55 μm.

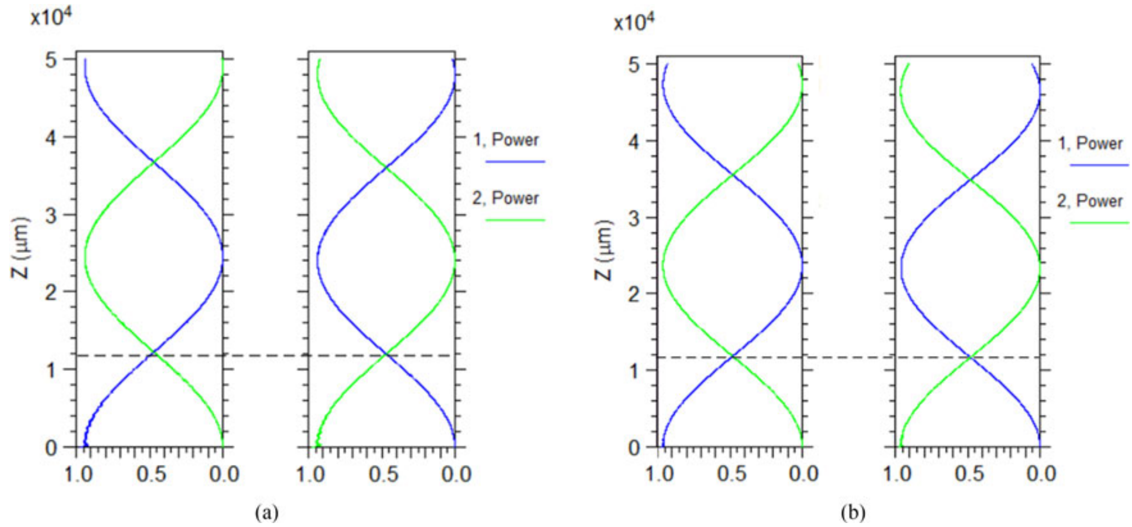

Fig. 8. Power evaluation of *x*-polarization (blue line) and *y*-polarization (green line) in core A (left) and B (right) at wavelength of 1.255 μm (a) and 1.725 μm (b).

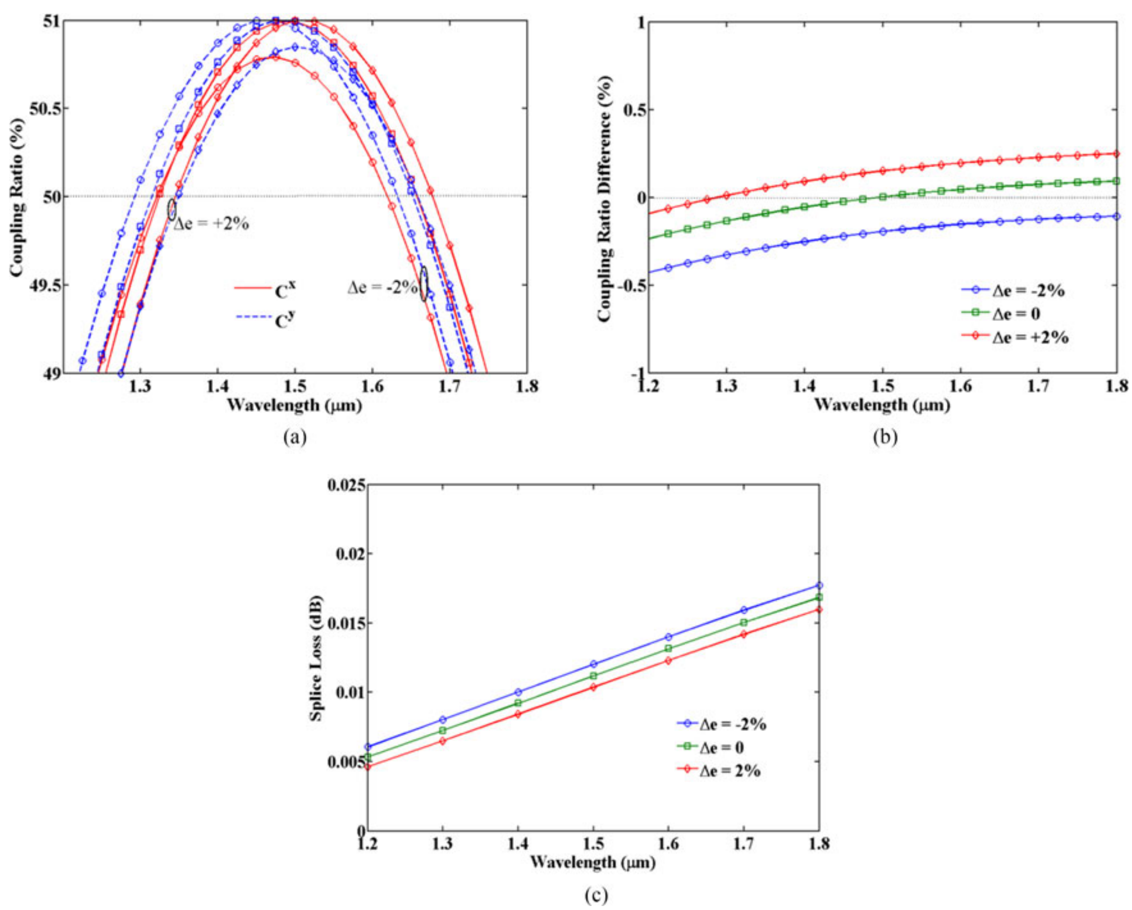

Fig. 9. Coupling ratio (a), coupling ratio difference (b), and splice loss (c) with different fabrication tolerance of ellipticity e.

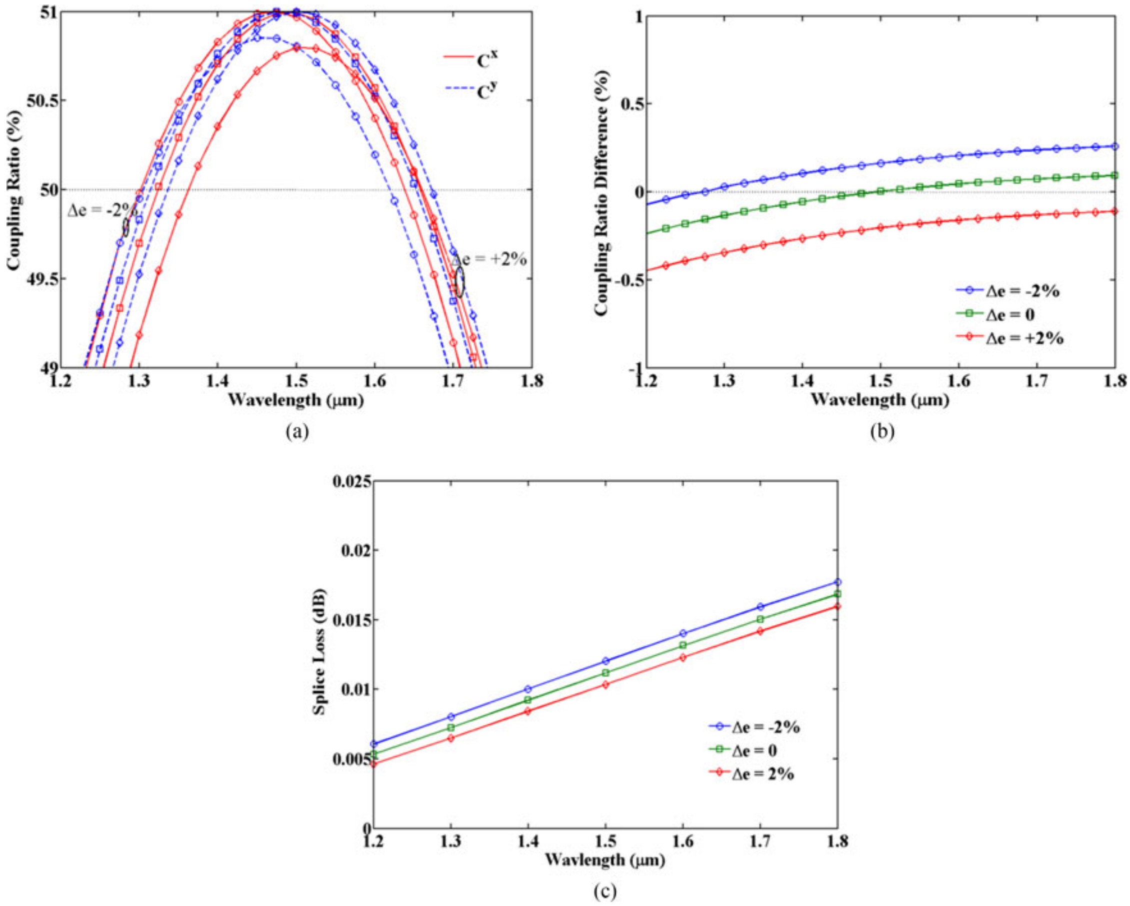

Fig. 10. Coupling ratio (a), coupling ratio difference (b), and splice loss (c) with different fabrication tolerance of ellipticity e.

11.6 mm along Z axis, the power of lights in *x*- and *y*-polarizations is almost equal in core A and B. It means that this designed fiber can achieve a broad bandwidth covers from 1.255 μm to 1.725 μm.

4. Discussion

In view of the fabrication feasibility and capability with SMFs, we design a PCF with uniform circular air holes in cladding and two fluorine-doped elliptical cores. Although the fabrication of elliptical fluorine-doped core is easier than elliptical air holes, the fabrication tolerance is necessary to be discussed. Air holes in cladding have no significant effects on fiber characteristics. Therefore, we focus on discussing the tolerance of elliptical core. First, the influence of the major axis radius is investigated. As shown in Fig. 9(a), the bandwidth has no significant changes and the peak of the coupling ratio shifts slightly when the ellipticity changes within $\pm$2%. Although the change of the ellipticity has no significant affection on the bandwidth, the difference of coupling ratio between two polarizations increases when ellipticity changes, but the coupling ratio difference is still lower than 0.5%. The splice loss becomes a little larger when ellipticity is decreased by 2%. This is because the mode field area narrows down with the decrease of the core size, but the splice loss is still less than 0.02 dB.

Then, we discuss the influence of the minor axis radius. The numerical results are shown in Fig. 10. The bandwidth becomes a little narrower and the peak of coupling ratio shifts slightly when the ellipticity changes within ±2%, and the coupling ratio difference becomes a little higher when the ellipticity changes, but it is also lower than 0.5%. The splice loss, caused by the mismatch of mode areas, is directly affected by the core size. The influence of minor axis radius is similar with major axis radius. The splice loss is lower than 0.02 dB when the ellipticity varies within ±2%. This means that the designed coupler has high fabrication tolerance.

5. Conclusion

We design a PCF with dual elliptical cores and uniform circular air holes in the cladding for directional coupler. Numerical results indicate that the coupling ratio of the proposed fiber can stay within 50 ± 1% in a broad bandwidth of 470 nm by using 11.6 mm long of the proposed PCF. The difference of coupling ratio between two polarizations is lower than 0.2% in the whole working wavelength range. In addition, the MFA of each core is around 70 μm^2, which make the splice loss caused by MFA mismatch is lower than 0.02 dB when the SMFs is used as input and output ports. Tolerance analysis results show the designed coupler has great fabrication feasibility. The designed PCF can be used as directional coupler in a high-rate, ultra-broadband communication system due to the high performance and low fabrication difficulty.

References

[1] F. Y. M. Chan and K. Yasumoto, "Design of wavelength tunable long-period grating couplers based on asymmetric nonlinear dual-core fibers," *Opt. Lett.*, vol. 32, pp. 3376–3378, 2007.

[2] B. H. Lee, J. B. Eom, K. S. Park, S. J. Park, and M. J. Ju, "Specialty fiber coupler: Fabrications and applications," *J. Opt. Soc. Korea*, vol. 14, pp. 326–332, Dec. 2010.

[3] C.-C. Wang and M.-H. Wang, "Broadband TE01 mode fiber coupler based on dual-core photonic crystal fiber," *Appl. Opt.*, vol. 53, pp. 7741–7748, 2014.

[4] P. Li and J. Zhao, "Polarization-dependent coupling in gold-filled dual-core photonic crystal fibers," *Opt. Exp.*, vol. 21, pp. 5232–5238, Mar. 2013.

[5] B. J. Mangan, J. C. Knight, T. A. Birks, P. S. J. Russell, and A. H. Greenaway, "Experimental study of dual-core photonic crystal fibre," *Electron. Lett.*, vol. 36, pp. 1358–1359, 2000.

[6] J. Lægsgaard, O. Bang, and A. Bjarklev, "Photonic crystal fiber design for broadband directional coupling," *Opt. Lett.*, vol. 29, pp. 2473–2475, 2004.

[7] S. K. Varshney, N. J. Florous, K. Saitoh, and M. Koshiba, "The impact of elliptical deformations for optimizing the performance of dual-core fluorine-doped photonic crystal fiber couplers," *Opt. Exp.*, vol. 14, pp. 1982–1995, 2006.

[8] S. Zhang *et al.*, "Theoretical study of dual-core photonic crystal fibers with metal wire," *IEEE Photon. J.*, vol. 4, no. 4, pp. 1178–1187, Aug. 2012.

[9] H. Wei, Y. Zhu, and S. Krishnaswamy, "Optofluidic photonic crystal fiber coupler for measuring the refractive index of liquids," *IEEE Photon. Technol. Lett.*, vol. 28, no. 1, pp. 103–106, Jan. 2016.

[10] S. Lou, Z. Tang, and L. Wang, "Design and optimization of broadband and polarization-insensitive dual-core photonic crystal fiber coupler," *Appl. Opt.*, vol. 50, pp. 2016–2023, May 2011.

[11] L.-W. Wang, S.-Q. Lou, W.-G. Chen, W.-L. Lu, and X. Wang, "Design and optimization of a novel broadband and polarization-insensitive dual-core photonic crystal fiber coupler over the whole optical communication band," *Acta Phys. Sinica*, vol. 61, Aug. 2012, Art.ID. 154207.

[12] X.-Y. Li, B. Sun, Y.-Y. Yu, and K.-P. He, "Bending dual-core photonic crystal fiber coupler," *Optik—Int. J. Light Electron Opt.*, vol. 125, pp. 6478–6482, 2014.

[13] H. Li, C. Xu, C. Tian, W. Wu, F. Xu, and B. Yu, "The asymmetric coupler based on the dual-core PCF," *Optik—Int. J. Light Electron Opt.*, vol. 127, pp. 694–696, 2016.

[14] G. Wang, Z. Wang, and F. Yu, "Design of single-polarization single-mode coupler based on dual-core photonic crystal fiber," *Opt. Eng.*, vol. 55, pp. 027101–027101, 2016.

[15] L. Xiao, M. S. Demokan, W. Jin, Y. Wang, and C.-L. Zhao, "Fusion splicing photonic crystal fibers and conventional single-mode fibers: Microhole collapse effect," *J. Lightw. Technol.*, vol. 25, no. 11, pp. 3563–3574, Dec. 2007.

[16] F. Brechet, J. Marcou, D. Pagnoux, and P. Roy, "Complete analysis of the characteristics of propagation into photonic crystal fibers, by the finite element method," *Opt. Fiber Technol.*, vol. 6, pp. 181–191, 2000.

[17] K. Saitoh, Y. Sato, and M. Koshiba, "Coupling characteristics of dual-core photonic crystal fiber couplers," *Opt. Exp.*, vol. 11, pp. 3188–3195, 2003.

[18] M. Koshiba, "Full-vector analysis of photonic crystal fibers using the finite element method(special issue on optical fibers and devices)," *IEICE Trans. Electron.*, vol. 85, pp. 881–888, 2002.

[19] S. Guenneu, A. Nicolet, F. Zolla, and S. Lasquellec, "Numerical and theoretical study of photonic crystal fibers," *Prog. Electromagn. Res.*, vol. 154, pp. 143–147, 2003.

[20] N. Florous, K. Saitoh, and M. Koshiba, “A novel approach for designing photonic crystal fiber splitters with polarization-independent propagation characteristics,” *Opt. Exp.*, vol. 13, pp. 7365–7373, 2005.
[21] J. H. Chong and M. K. Rao, “Development of a system for laser splicing photonic crystal fiber,” *Opt. Exp.*, vol. 11, pp. 1365–1370, 2003.
[22] B. J. Mangan, J. Arriaga, T. A. Birks, J. C. Knight, and P. S. J. Russell, “Fundamental-mode cutoff in a photonic crystal fiber with a depressed-index core,” *Opt. Lett.*, vol. 26, pp. 1469–1471, 2001.
[23] F. Fogli, L. Saccomandi, P. Bassi, G. Bellanca, and S. Trillo, “Full vectorial BPM modeling of index-guiding photonic crystal fibers and couplers,” *Opt. Exp.*, vol. 10, pp. 54–59, 2002.